Organic Process Research & Development **2006**, *10,* 739–750

Process Modelling Tools for Continuous and Batch Organic Crystallization Processes Including Application to Scale-Up

E. Kougoulos,[†,§] A. G. Jones,[†] and M. W. Wood-Kaczmar*[,‡]

Department of Chemical Engineering, UCL, Torrington Place, London WC1E 7JE, U.K., and Strategic Technologies, GSK Medicines R&D, Gunnels Wood Road, Stevenage SG1 2NY, U.K.

Abstract:

Computational fluid dynamics (CFD) is a powerful simulation tool that was successfully used to investigate mixing, turbulence, and shear in a laboratory-scale MSMPR and batch cooling crystallizer for an organic fine chemical. CFD gives a qualitative engineering insight into the effects of the impeller configuration on the crystallization rates and particle size distribution. A process-modelling tool, gPROMS (Process Systems Enterprise), was used to model particle size and size distribution in both batch and continuous laboratory-scale crystallization processes with predictive simulations in good agreement with experimental results. CFD simulations of large-scale crystallizations using constant specific power input per unit mass, predict an increase in macromixing and decrease in micromixing and turbulence. This effect should improve process performance of batch cooling crystallizers on scale-up including the product quality of the final solid form in terms of the particle size and crystal habit. This is due to improved suspension mixing and secondary nucleation effects and attrition decreasing with scale-up. CFD heat transfer simulations, however, predict varying temperature profiles together with less efficient heat transfer with the presence of distinct cooling zones, which can degrade product performance in terms of encrustation and agglomeration resulting in wider particle size distributions.

1. Introduction

Crystallization is one of the most critical steps used in the pharmaceutical industry. The processing performance and quality of organic fine chemicals such as filterability, drying, and compressibility are determined by the particle size distribution, morphology, purity, yield, and selectivity. The scale-up and modelling of crystallization processes are some of the most challenging tasks in the pharmaceutical industry.

The main challenge involved in the design of industrial pharmaceutical crystallizers is to predict the influence of vessel geometry, configuration, operating conditions, and the effects of scale on the process behaviour, particle quality, and particle size distribution. Industrial crystallizer design is hindered by the lack of rational scale-up rules and incorporation of hydrodynamic information and kinetics. These problems of scaling up are further compounded by the limited quantities of material are available in the early stages of process development. This has the effect of limiting the number of scale-up experiments that can be performed, and due to time and resource constraints it is challenging to achieve a robust process development route.

The conventional approach to scale-up is based on the principle of similarity, which is aimed at maintaining similarity of equipment, flow characteristics, specific power input, and temperature profiles. The maintenance of geometrical similarity requires identical ratios of corresponding dimensions in two scales. Geometric similarity is assessed by the tank height-to-diameter ratio including impeller-to-tank diameter ratio. However, the exact scale-up of continuous and batch crystallizers is not possible because it would be necessary to preserve similar flow characteristics of both the solid and liquid phases together with identical temperature and supersaturation profiles in all regions. The most commonly used scale-up criteria include constant agitator tip speed, constant power input per unit mass, constant Reynolds number, and constant agitator speed. In processes such as batch cooling and continuous crystallizations, where the crystallization rate is controlled by the degree of mixing and heat and mass transfer, these simple scale-up criteria often fail. Computational fluid dynamics (CFD) is a process-modelling tool[13] that can be used to gain a valuable quantitative insight into mixing, turbulence, and heat transfer within agitated vessels that would be difficult to obtain experimentally. CFD modelling of mixing and turbulence in stirred tanks has been comprehensively investigated.[1−5] Maggiorios et al.[6] successfully used CFD to model particle size in suspension polymer reactors. Micale et al.[7] and Montante et al.[8] have recently developed the multi-fluid model (MFM) to model dilute particle suspensions with monodisperse particle sizes in agitated vessels. CFD mod-

* Corresponding author. Telephone: +44 (0) 207 679 3828. Fax: +44 (0) 20 7383 2348.

[†] Department of Chemical Engineering, UCL.

[‡] Strategic Technologies, GSK Medicines R&D.

[§] Current address: Pfizer Limited, Ramsgate Road, Sandwich, Kent CT16 9NJ, U.K.

(1) Ranade, V. V. *Chem. Eng. Sci.* **1997**, *52*, 24, 4473−4484.
(2) Sahu, A. K.; Kumar, A.; Patwardhan, A. W.; Joshi, J. B. *Chem. Eng. Sci.* **1999**, *54*, 13−14, 2285−2293.
(3) Montante, G.; Lee, K. C.; Brucato, A.; Yianneskis, M. *Comput. Chem. Eng.* **2001**, *25*, 4−6, 729−735.
(4) Montante, G.; Lee, K. C.; Brucato, A.; Yianneskis, M. *Chem. Eng. Sci.* **2001**, *56*, 12, 3751−3770.
(5) Baccar, M.; Kchaou, H.; Mseddi, M.; Abid, M. S. *Mec. Ind.* **2003**, *4*, 3, 301−318.
(6) Maggiorios, D.; Goulas, A.; Alexopoulos, A. H.; Chatzi, E. G.; Kiparissides, C. *Comput. Chem. Eng.* **1998**, *22*, 1, S315−S322.
(7) Micale, G.; Montante, G.; Magelli, F.; Brucato, A. 10th European conference on mixing, Delft, The Netherlands, 2000; pp 125−132.
(8) Montante, G.; Micale, G.; Magelli, F.; Brucato, A. *Trans. Inst. Chem. Eng.* **2001**, *79*, A8, 1005−1010.

10.1021/op060039+ CCC: $33.50
Published on Web 05/10/2006

elling of heat transfer using different vessel and impeller configurations has also been successfully investigated.[9−12]

CFD has been used to determine shear distribution and mixing profiles, whereby qualitative or semiquantitative information (by including hydrodynamic influences) is used for scaling up organic crystallization processes. This approach, however, cannot guarantee a "right first time" approach to scale-up. It is essential to combine hydrodynamic information with crystallization kinetics. Schmidt et al.[14] have made an important step in this direction by using CFD, simplified growth kinetics, and solubility characteristics to scale-up crystallization processes. Urban and Liberis[15] have used a hybrid gPROMS/CFD approach for steady-state forced cooling crystallizers, and Bezzo et al.[48,49] used an automatic zoning technique to develop a compartmentalised approach. Recently, secondary nucleation and attrition,[16] which are dominant in batch cooling suspension crystallization processes has been taken into account in the process modelling aspects. There has been little focus in industry on determining and combining crystallization kinetics, particularly secondary nucleation rates, with computational fluid dynamic information via process modelling tools such as gPROMS[17] (Process Systems Enterprise Ltd., www.psenterprise.com).

The crystallization kinetics,[18] solubility[19] and polymorphism[20] characteristics of organic chemical compounds are critical for the prediction of scale-up behaviour. Control of polymorphism and crystal morphology is a major objective in crystallization process design. Another objective is to design a robust crystallization scale-up process scaled up from laboratory- to a pilot-plant scale and finally to manufacturing scale. This requires a crystallization process in which batch-to-batch variations and fines production is minimised. During scale-up, hydrodynamic phenomena influence the rates and, in particular, growth and nucleation on a localised scale within a crystallizer and thereby also affect the final product performance. The hydrodynamic effects are linked to mixing, turbulence, and heat transfer. These can all be investigated using CFD and must be considered for successful scale-up process development. To achieve quantitative scale-up, localised hydrodynamic information obtained via CFD must be combined with kinetics and solubility data via a compartmental modelling approach[21] that is based on heuristics.[22] gPROMS is a dynamic and steady-state process modelling tool[17] that can be used to simulate particulate processes whereby crystallization kinetics, thermodynamics, and solubility characteristics are introduced within a population, mass, momentum, and energy balances.

For successful scale-up, it is important to ensure geometrical similarity in crystallization vessels, including baffles and impellers, from laboratory- to pilot-plant scale based on the mixing concepts of power input, suspension, shear, energy dissipation, and heat transfer. Each of these requires different scale-up criteria depending on the agitation speed. However, keeping one scale-up criterion constant violates another.[23] Using a constant specific power input per unit mass leads to improved mixing characteristics in terms of particulate suspension upon scale-up. This allows for improved homogeneity, leading to more uniform growth. In addition, the tip speed is reduced, resulting in a reduction in the local energy dissipation and shear rate. This results in a reduction in fines and less particulate attrition in crystallization processes. This should allow for an improvement in downstream processing such as filtration and drying. However, in batch cooling crystallizations, the heat transfer becomes less efficient upon scale-up, resulting in variable particle size distributions. To achieve similar heat transfer, the process and operating conditions have to be altered by either increasing the cooling rate or process time. The former may result in large, localised, wall temperature gradients and consequent encrustation.

This paper reports an investigation into the use of CFD and gPROMS as process modelling tools to model hydrodynamics and predict particle size distributions for a laboratory-scale batch and continuous mixed suspension mixed product removal (MSMPR) crystallizer, respectively. In particular, the effects of impeller type and velocity influencing the crystallization rates and the extent of solid−liquid phase mixing are considered. Furthermore, predictive CFD simulations are used for scale-up studies to investigate solid−liquid phase mixing, turbulence, and heat transfer. This is performed to provide a qualitative insight for the failure of common scale-up criteria when applied to organic batch cooling suspension crystallization processes. To illustrate the above, three case studies will be considered.

2. Theory

2.1. Physical Aspects. Using geometrically similar agitated crystallization vessels allows dimensional analysis to be used to describe the power requirements of the system. The dimensionless terms typically associated with momentum transfer are described. The Reynolds number describes the ratio of inertial to viscous forces prevailing in crystallizers and is given by,

(9) Baccar, M.; Abid, M. S. *Int. J. Therm. Sci*. **1999**, *38*, 10, 892−903.
(10) Delaplace, G.; Torrez, C.; Lueliet, J. C.; Belaubre, N.; Andre, C. *Trans. Inst. Chem. Eng.* **2001**, *79*, 927−937.
(11) Baccar, M.; Kchaou, H.; Mseddi, M.; Abid, M. S. *Int. J. Therm. Sci.* **2001**, *40*, 8, 753−772.
(12) Yapici, H.; Basturk, G. *Comput. Chem. Eng.* **2004**, *28*, 11, 2233−2244.
(13) Versteeg, H. K.; Malalasekera, W. *An introduction to Computational Fluid Dynamics: The Finite Volume Method*, 1st ed.; Longman Scientific & Technical: Harlow, Essex, England, 1995.
(14) Schmidt, B.; Patel, J.; Ricard, F. X.; Brechtelsbauer, C. M.; Lewis, N. *Org. Process Res. Dev.* **2004**, *8*(6), 998−1008.
(15) Urban, Z.; Liberis, L. *Hybrid gPROMS-CFD*. Modelling of an industrial scale crystalliser with rigorous crystal nucleation and growth kinetics and a full population balance; Chemputers: Dusseldorf, Germany, 1999.
(16) Kougoulos, E.; Wood-Kaczmar, M. W.; Jones, A. G. *Powder Technol.* **2005**, *155*, 153−158.
(17) Pantelides, C. C.; Oh, M. *Powder Technol.* **1996**, *87*, 1, 13−20.
(18) Kougoulos, E.; Wood-Kaczmar, M. W.; Jones, A. G. *J. Cryst. Growth* **2005**, *273*, 3−4, 520−528.
(19) Thompson, D. R.; Kougoulos, E.; Wood-Kaczmar, M. W.; Jones, A. G. *J. Cryst. Growth* **2005**, *276*, 1−2, 230−236.
(20) Beckmann, W. Pharmaceutical Crystallisation: Polymorphs, Pseudo- Polymorphs and Particle Formation, 15th Industrial Symposium on Industrial Crystallization, 2002.
(21) Kougoulos, E.; Wood-Kaczmar, M. W.; Jones, A. G. *Trans IChemE, Part A: Chem. Eng. Res. Des.* **2005**, *83* (A1), 30−39.
(22) Rigopoulos, S.; Jones, A. G. *Chem. Eng. Sci.* **2003**, *58*, 14, 3077−3089.
(23) Zlobarnik, M. *Scale-up in Chemical Engineering*; Wiley-VCH: New York, 2002.

$$\{Re\} = \frac{\rho_F N d_i^2}{\mu} \quad (1)$$

The power number is given by,

$$Po = \frac{P}{\rho_F N^3 d_i^5} = \frac{2\pi NM}{\rho_f N^3 d_i^5} \quad (2)$$

where P is the power drawn by the agitator and ρ_f is the slurry density. In agitated crystallizers fully turbulent flow is produced at $Re > 20\,000$ with $Po =$ constant. The power number value depends on the impeller type and is independent of scale, providing that geometric similarity is maintained.

For constant power for different scales of operation with geometric similarity, the following impeller pumping flowrate relationship is used,

$$Q_p \propto N d_i^3 \quad (3)$$

Hence, large impeller diameters produce high volumetric pumping flow rates. To maintain a constant turnover time upon scale-up, a constant stirrer speed is used.

2.2. Mixing. To achieve the homogeneous growth of particles, all must be suspended in the mother liquor to provide the maximum surface area and homogeneous conditions for mass transfer from the solute to the solid phase. A complete suspension is achieved by using the Zwietering[24] "just suspension speed", as the minimum impeller speed necessary at which all particles are suspended off the bottom of the crystallizer or when residence times are less than 2 s.[24]

$$N_{js} = s\upsilon^{0.1}\left(\frac{g\Delta\rho}{\rho_l}\right)^{0.45} X^{0.13} d_p^{0.2} D^{-0.85} \quad (4)$$

If the crystals are not fully suspended, a widening of the particle size distribution can be expected due to agglomeration and encrustation. An agitator speed or different impeller configuration above the just suspended speed may have limited mass transfer[25] benefits but ensures that particles are homogeneously distributed throughout the vessel. In batch crystallizations, there is another complication associated with the homogeneity of the particles. This is due to a continual change with respect to the particle concentration throughout the crystallization process as a result of particulate growth.

The hydrodynamics conditions within a batch crystallization vessel vary from one location to another, in terms of macromixing and micromixing. Macromixing occurs on a large scale and is mainly backmixing due to convection motion and is defined by a circulation time as follows,

$$t_{circ} = \frac{V}{Q_p} = \frac{V}{Fl \cdot N \cdot d_i^3} \quad (5)$$

Micromixing however comprises the viscous, convective deformation of fluid elements, followed by molecular diffusion on the Kolmogorov scale, which is determined by the eddy size. The rate of micromixing depends on the local rate of dissipation of the turbulent energy especially in the impeller region. The local rate of energy dissipation affects the crystallization rates. According to Baldyga and Bourne,[26] the characteristic time for micromixing can be related to the engulfment rate [E] and thus to the turbulent energy dissipation rate,

$$t_{micro} = E^{-1} = 17.2\left(\frac{\epsilon_{loc}}{\nu}\right)^{-0.5} \quad (6)$$

In reactive precipitation processes, micromixing is the controlling mechanism.[27] Hence, localised values for the energy dissipation rate and the addition point will determine the reaction rate and, hence, final product performance. For macromixing processes, the macromixing time needs to be kept constant upon scale-up and is achieved with constant agitator speed. Although the suspension mixing is improved, there is a competing mechanism with attrition, and this may lead to the production of fine particles during the crystallization process. This has the effect of reducing filtration efficiency, with increased filtration times and filter blinding.

2.3. Heat Transfer. In agitated batch cooling crystallizations, it is important that homogeneous heat transfer occurs throughout the vessels, by ensuring that no temperature gradients or local cooling zones exist. High temperature gradients can result in wall encrustation leading to severe agglomeration effects and/or different supersaturation profiles in the bulk and at the wall. CFD can be used to provide a valuable insight into heat transfer and will be briefly illustrated in this paper.

Using dimensional analysis, the following heat transfer correlation can be used to model the liquid side heat transfer coefficient in batch cooling suspension crystallization vessels as follows,

$$Nu = C \cdot Re^{0.67} \cdot Pr^{0.33} (\mu/\mu_w)^{0.14} \quad (7)$$

where

$$C = f(\text{geometry and flow regime}) \quad (8)$$

At constant energy dissipation and geometrical similarity the heat transfer coefficient relationship is as follows,

$$h \propto d_i^{-1/9} \quad (9)$$

The heat transfer of the bulk volume depends on the specific heat capacity and must also be taken into account rather than just the heat transfer at the wall. Moreover, the heat transfer coefficient is reduced when scaling up with constant specific power input per unit mass because the ratio of heat transfer area to reaction volume decreases significantly.

2.4. Constant Specific Power Input per Unit Mass. This scale-up criterion is most commonly used in mixing limited unit operations and is based on constant mean energy dissipation rate per unit mass as follows,[28]

(24) Zwietering, T. N. *Chem. Eng. Sci.* **1958**, 244−253.
(25) Nienow, A. W.; Miles, D. *J. Chem. Eng.* **1978**, *15*, 13.
(26) Baldyga, J.; Bourne, J. *Turbulent Mixing and Turbulent conditions*; Wiley: England, 1999.
(27) Zauner, R.; Jones, A. G. *Chem. Eng. Sci.* **2002**, *57*, 5, 821−831.

$$\epsilon_{av} = \frac{P}{\rho_F \cdot V} = \frac{P_o \cdot \rho_F \cdot d^5 \cdot N^3}{\rho_F \cdot V} = constant \quad (10)$$

In micromixing-controlled processes such as reactive and anti-solvent precipitations, the local energy dissipation rate will dominate the nucleation rate and, hence, particle formation at the anti-solvent or reactant addition point. For macromixing-controlled crystallizations processes such as batch and continuous, the local energy dissipation rate must be constant upon scale-up. High dissipation rates may result in increased fines formation, whereas low values may result in poor particulate suspension and agglomerated particles.

2.5. Solubility and Supersaturation. Crystallization kinetics including rates of nucleation, crystal growth, attrition, and agglomeration are dependent on the supersaturation levels and therefore determine the particle size distribution and product performance. The accurate measurement of supersaturation is fundamental to the modelling of batch cooling crystallizations.[29−34] ATR−UV spectroscopy has been used as an on-line monitoring tool[19] to determine accurate equilibrium solute concentrations and to develop a solubility model for both batch and continuous crystallization processes as a function of temperature for the organic fine chemical under investigation as follows,

$$C_{eq}[T] = 3.5e^{-03} \exp^{4.44e^{-02}T} \quad (11)$$

2.6. Crystallization Kinetics. To predict the crystallization behaviour of a batch cooling or continuous crystallization processes upon scale-up, the crystallization kinetics[35−38] can be determined on a laboratory scale using population balance techniques[43] coupled with hydrodynamic information obtained from CFD simulations for scale-up purposes. For the organic fine chemical investigated, complex kinetic models for size-dependent growth and total nucleation were developed,

$$G(L) = k_g\sigma(1 - \exp[-17400(L + 1e^{-07})]) \quad \text{for} \quad L \le 200\,\mu\text{m} \quad \text{and} \quad 0.45 \le \sigma \le 1.2 \quad (12)$$

$$L > 200\,\mu\text{m}, \quad G \rightarrow G_e \quad (13)$$

The total nucleation rate for a crystallizer equipped with a pitch blade impeller is described as a function of the average energy dissipation, average growth rate, and suspension density as follows,

$$B_{TOT} = (1.0 \times 10^{19}) M_T^{1.55} G_{av}^{1.2} \epsilon^{0.2} \quad (14)$$

The average growth rate is a function of the relative supersaturation and is given as follows,

$$G_{av} = k'_g \sigma^{1.28} \quad (15)$$

The average growth is based on the assumption that particles are removed from the continuous crystallizer on average within 1 mean residence time.

The total nucleation rate for a crystallizer equipped with either a pitch blade or flat blade impeller is described as a function of the suspension density and relative supersaturation levels as follows,

$$\text{pitch blade impeller} \quad B_{TOT} = (4 \times 10^{09}) M_T^{1.57} \sigma^{2.64} \quad (16)$$

$$\text{flat blade impeller} \quad B_{TOT} = (2 \times 10^{09}) M_T^{1.64} \sigma^{2.93} \quad (17)$$

3. Results and Discussion

3.1. Case Study I: Laboratory-Scale MSMPR Crystallizer. In this case study, the continuous crystallization of an organic fine chemical in a 0.5-L laboratory scale using a mixed suspension mixed product removal (MSMPR) crystallizer with product recycle[39] will be considered. The key aim of this study was to determine the influence of the impeller configuration on the crystallization kinetic phenomena. Furthermore, the extent of solid−liquid phase mixing is also considered. The crystallization kinetics developed from the continuous MSMPR crystallizer, in particular the total nucleation rate, influences the particle size distribution and product performance significantly. Continuous MSMPR experiments[18] have shown that the impeller type influences the mass transfer characteristics, secondary nucleation, and attrition of the crystallization system under investigation. The capability of gPROMS as a modelling tool for predicting the particle size distribution is illustrated and compared to experimental continuous MSMPR crystallizations.

3.1.1. Experimental Set-Up. The two impeller types considered were a four-bladed 45° pitch blade impeller (d_i = 45 mm) and a two-bladed flat blade impeller (d_i = 60 mm). The continuous MSMPR crystallizer equipped with a flat blade impeller contained no baffles, whereas with a pitch blade impeller three baffles were used to provide axial and radial flow. An initial solute concentration of 4% w/w and variable mean residence times were used for both impeller configurations. Agitator rates of 300, 400, 500, and 600 rpm were used, respectively. The MSMPR crystallizer was operated at a constant temperature of 29 °C until steady-state operation was achieved. Steady-state operation was achieved after 6−8 residence times. A Lasentec FBRM instrument was used on-line and in real time to monitor the chord length distribution[39] as a process analytical technique (PAT) during the crystallization process and to determine the point at which steady-state operation is achieved. The

(28) Harnby, N.; Edwards, M. F.; Nienow, A. W. Mixing in the Process Industries. 2nd ed.; Butterworth-Heinemann: Woburn, MA, 1992.
(29) Groen, H.; Roberts, K. J. *Cryst. Growth Des.* **2004**, *4*, 929.
(30) Groen, H.; Roberts, K. J. Proceedings of the Fifth International Workshop on the Crystal Growth of Organic Materials (CGOM-5); IChemE, Cambridge, UK, ISBN 0 85295 4247, 1999.
(31) Lewiner, F.; Klein, J. P.; Puel, F.; Conesa, G.; Fevotte, F. *Chem. Eng. Sci.* **2001**, *56*, 6, 2069−2084.
(32) Togkalidou, T.; Fujiwara, M.; Patel, P.; Braatz, R. D. *J. Cryst. Growth* **2001**, *231*, 4, 534−543.
(33) Derdour, L.; Feroutte, F.; Peul, P.; Ceurin, P. *Powder Technol.* **2003**, *129*, 1−7.
(34) Groen, H.; Borissova, A.; Roberts, K. J. *Ind. Eng. Chem. Res.* **2003**, *42*, 1, 198−206.
(35) Zauner, R.; Jones, A. G. *Chem. Eng. Sci.* **2000**, *55*, 4219−4232.
(36) Tanrikulu, S. U.; Eroglu, A. N.; Bulutchu, A. N.; Ozkar, S. *J. Cryst. Growth* **2000**, *208*, 533−540.
(37) Sha, Z. L.; Hatakka, H.; Louhi-Kultanen, M.; Palosaari, S. *J. Cryst. Growth* **1996**, *166*, 1105−1110.
(38) Chen, M. R.; Larson, M. A. *Chem. Eng. Sci.* **1985**, *40*, 1267−1294.
(39) Kougoulos, E.; Jones, A. G.; Jennings, K. H.; Wood-Kaczmar, M. W. *J. Cryst. Growth* **2005**, *273*, 3−4, 529−534.

Table 1. **Mixing characteristics of the MSMPR crystallizer equipped with flat blade and pitch blade impellers operating at 300 rpm**

	flat blade	pitch blade
tip speed [m/s]	1.02	0.72
Re	7190	3600
Q_p [m^3/s]	3.07×10^{-4}	1.67×10^{-4}
t_{circ} [s]	1.79	3.29
Po	0.76	1.24
P [W]	0.09	0.03
t_{micro} [s]	3.7	6.72
ϵ_{av} [W/kg]	0.19	0.09

steady-state supersaturation levels were determined using off-line HPLC analysis.

3.1.2. CFD Simulations and Mixing. To provide an explanation for the differences observed in the nucleation rates and particle size distributions using either a pitch blade or a flat blade impeller at 300 rpm, predictive CFD simulations using CFX-Promixus (AEA Technology, Harwell)[40] were carried out to provide a qualitative insight. A liquid phase (mother liquor) was used to determine the effects of the shear rate distribution and mixing profiles at a constant agitation rate of 300 rpm on the crystallization kinetics. The express option of the software automatically sets up and performs a three-dimensional hexahedral element-based finite volume. CFD simulations were also extended to include a solid−liquid phase using CFX v.4 (AEA Technology, Harwell) to determine the extent of particulate suspension within the continuous crystallizer operating at 300 rpm. The multiple frames of reference (MFR) technique was used to simulate the impeller rotation.[41] The sliding grid (mesh)[13] technique, although being a more accurate method, is computationally more expensive when compared to the MFR technique. CFD simulations predict that the overall flow patterns produced using either a pitch blade or a flat blade impeller are significantly different. Table 1 summarises the mixing and turbulence characteristics using eqs 2 and 3 and 5 and 6. CFD simulations predict a vortex effect and radial flow (Figure 2d), when the flat blade impeller is used in the continuous crystallizer. Similarly, with a pitch blade impeller, lower flow velocities and axial flow (Figure 2a) are observed with the vortex formation eliminated due to the presence of baffles providing a stabilisation mechanism.

Higher velocities are achieved by using the flat blade at the same impeller velocity due to the increased power input; however, limited mass transfer benefits result in terms of growth rates. The mass transfer coefficients (k_g) estimated from MSMPR experiments for flat blade and pitch blade impellers are 3.26×10^{-08} m/s and 3.06×10^{-08} m/s, respectively. The mass transfer coefficients for both impeller types were determined by fitting eq 12 to the experimental growth rates versus relative supersaturation levels. A series of experiments were carried out over a range of relative supersaturation levels.[50] Results indicated that the type of impeller used may affect the mass transfer (diffusion step) rate of crystal growth but not significantly in this case, as the accuracy due to experimental fitting must also be taken into account.

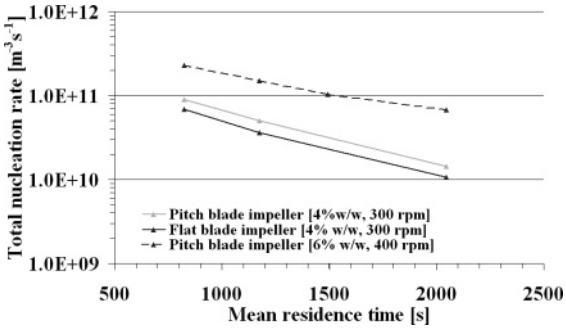

Figure 1. **Nucleation rates based on using pitch blade and flat blade impellers versus the mean residence time.**

Figure 1 shows the total nucleation rates estimated from the experimental steady-state particle size distributions as a function of the mean residence time using the different impeller types at 300 rpm from the continuous MSMPR crystallizer. The continuous crystallizer equipped with a pitch blade impeller produces higher nucleation rates when compared to those with the flat blade impeller.

CFD simulations indicate that the impeller geometry and type have a significant effect on the shear rate and energy dissipation distribution profile. A high shear region (shown in pink) is predicted from CFD simulations in the impeller zone for both impeller types, including wall shear (panels b and e of Figure 2). In addition to this observation, a low shear rate distribution (shown in blue) is observed in the upper regions with the MSMPR crystallizer equipped with a pitch blade impeller and a moderate normalised shear distribution (shown in green) for a flat blade impeller.

Further experimental investigations, based on the impeller geometry and material properties of the organic fine chemicals, were also carried out to determine the contributions of turbulent shear and impeller contacts on the attrition and total nucleation rates.[42] Figure 3 shows that impeller contacts contribute to the majority of attrition fragments and, hence, influence the secondary nucleation much more significantly than when compared to turbulent shear. The CFD predictions, in addition to the above observations, suggest that, due to the pitch blade impeller having four 45° angled blades rather than two flat blades, there is a higher probability of attrition events due to particle−impeller contacts and higher secondary nucleation rates being evident. This occurs even though the flat blade impeller operates at a higher tip velocity and produces higher maximal and average energy dissipation rates.

One of the main MSMPR assumptions is based on the laboratory-scale crystallizer being well mixed.[43] Two-phase mixing was investigated within the laboratory-scale MSMPR crystallizer using CFX-4 (AEA Technology, Harwell) to evaluate the assumption that the hydrodynamics should influence the crystallization kinetics at a minimum. To assess

(40) *CFX-Promixus*_2.1 Manual; AEA Technology: Harwell: UK, 2000.
(41) Lane, G. L.; Schwarz, M. P. CFD Modelling of Gas-Liquid Flow in Stirred Tank. *Chemeca '99*, Newcastle, Australia, 1999.
(42) Synoweic, P.; Jones, A. G.; Shamlou, P. A. *Chem. Eng. Sci.* **1993**, *48*, 3485−3495.
(43) Randolph, A. D.; Larson, M. A. *Theory of Particulate Processes*, 2nd ed.; Academic Press: New York, 1988.

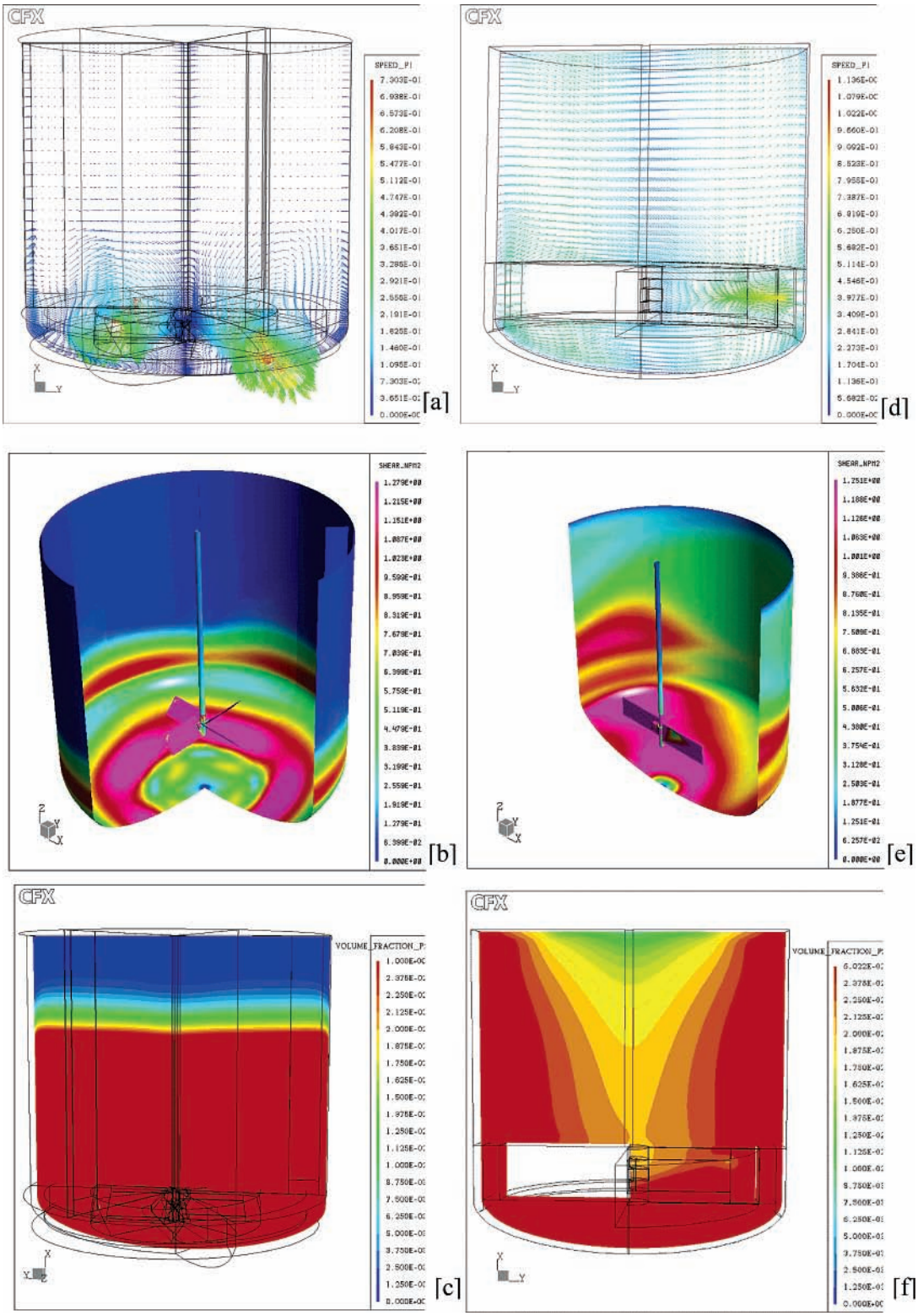

Figure 2. **Velocity [m/s], normalised shear, and solids volume fraction (maximum solids hold-up) distribution respectively (a−c) pitch blade and (d−f) flat blade impeller.**

the mixing in the crystallization process, several assumptions were made on the process physical properties.

1. The Multi-Fluid model (MFM)[44] with a modified drag coefficient[45] was assumed to be applicable for mean particle sizes of 100 μm and 75 μm for a flat blade impeller and pitch blade impeller, respectively.

2. The experimental crystal shape is paralleliped, but the particles within CFD were assumed to be spherical. Current

(44) Micale, G.; Montante G.; Magelli, F.; Brucato, A. CFD simulation of particle distribution in a multi-impeller high aspect ratio stirred vessel. 10th European conference on mixing. Delft, The Netherlands, 2000; pp 125−132.

(45) Brucato, A.; Grisafi, F.; Montante, G. *Chem. Eng. Sci.* **1998**, *53*, 3295−3314.

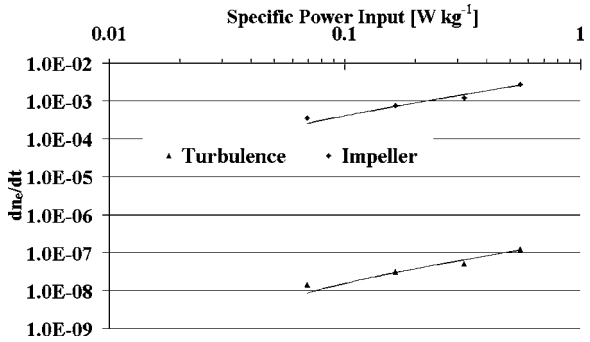

Figure 3. **Net attrition rate contribution based on impeller and turbulence shear using a pitch blade impeller.**

models to simulate solid−liquid phase mixing in CFD have not been developed to account for the irregular shapes of most organic compounds and the suspension of these particles in solution.[46]

3. The crystal density was determined to be 1400 kg m^{-3}. CFD predictions (panels c and f of Figure 2) show that in the MSMPR crystallizer equipped with a flat blade, a homogeneous uniform suspension is achieved; however, as expected, there is a concentration gradient with a predicted solids vortex produced in an axial direction near the shaft. In the MSMPR equipped with a pitch blade impeller a complete suspension is achieved, but in the upper region a clear mother liquor region is evident. In reality, however, this region will contain fine particles less than 75 μm. This zone will also contain fewer (number and mass) particles than in the bulk or below the impeller, which is a high solids concentration zone and is also observed during experimentation. CFD can be used to model polydisperse particle sizes, but excessive computational requirements are needed. Process development requires a CFD process simulation output within days rather than months as there is often a requirement to scale up pharmaceutical crystallization unit operations within 4 to 8 weeks.

The Zwietering correlation (eq 4) was used to estimate the just suspended speed for the pitch blade and flat blade impellers. This was determined to be 300 and 200 rpm for the pitch blade impeller and flat blade impeller, respectively, to achieve a complete suspension. The just suspended speed can be multiplied by a safety factor of 1.3−1.5 to achieve a homogeneous suspension. For example, to achieve a homogeneous suspension in the continuous crystallizer equipped with either a pitch blade or a flat blade impeller, an agitator speed of around 400 and 250 rpm, respectively, will be necessary.

3.1.3. gPROMS Simulation Predictions. gPROMS was used as a process simulation tool to predict the steady crystal size distributions based on crystallization kinetics and solubility data using eqs 11−17. The population and mass balance for continuous crystallizations was also implemented into the simulation model. The simulations were run until steady state was obtained. The Lasentec FBRM chord measurements were discretised into 252 logarithmic channels and converted to a particle size (mass) distribution. The

(46) Wei, D. Mixing reactions: CFD and reactor design. *Chem. Eng*. **2005**, 19−21.

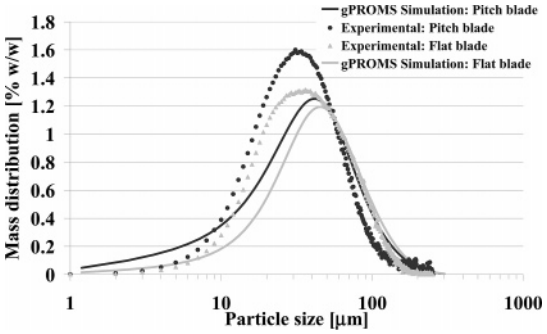

Figure 4. **Experimental and gPROMS-simulated steady-state continuous particle size distributions based on two different impeller types using a residence time of 825 s.**

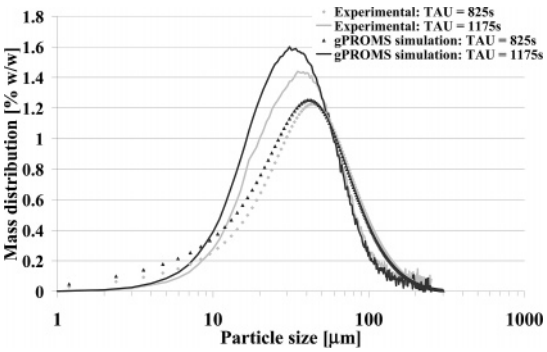

Figure 5. **Experimental and gPROMS-simulated steady-state continuous particle size distributions based on using different mean residence times (pitch blade impeller).**

gPROMS simulations of the particle size distribution were also expressed in 252 logarithmic intervals. Figure 4 shows the experimental and predicted particle size distributions (from gPROMS simulations) obtained using the two different impeller types using a mean residence time of 825 s.

Figure 5 shows the experimental and predicted particle size distributions (from gPROMS simulations) using different mean residence times for a pitch blade impeller. The trend observed in the simulated and experimental distributions (Figure 4) is as expected because the total nucleation rate using a flat blade impeller is less than that of a pitch blade impeller, thus allowing for the growth of larger particles. The simulations overestimate the crystal size distribution for both impeller configurations. The difference in the crystal size distributions is due to the fact that particulate attrition is not taken into account. The experimental volume mean size is 57 and 61 μm for a pitch blade impeller and a flat blade impeller, respectively. Albeit that attrition is not taken into account, the experimental results compare well to the simulated volume mean size values of 60 and 65 μm, respectively. The trends in the simulated and experimental results (Figure 5) are as expected as longer residence times correspond to longer periods over which particle growth takes place, resulting in the formation of large crystals corresponding to a shift to the right in the CSD. The experimental and simulated results compare well as the volume mean sizes for a mean residence time of 1175 s are 71 and 60 μm, respectively, for simulated and experimental results.

Further experiments were carried out in the continuous MSMPR crystallizer equipped with a pitch blade impeller

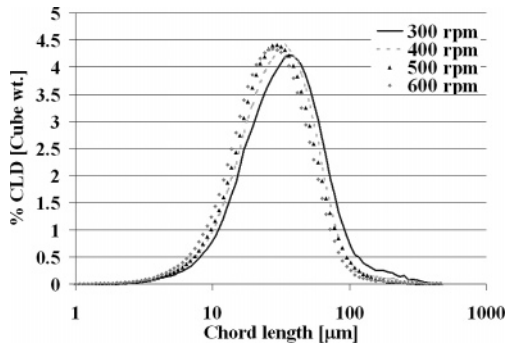

Figure 6. **Particle size distribution shift due to the increase in agitator speed (pitch blade impeller).**

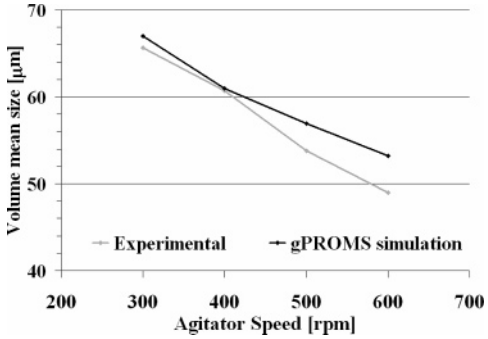

Figure 7. **Experimental and gPROMS-simulated steady-state volume mean sizes as a function of agitator speed (pitch blade impeller).**

to determine the effects of increasing the agitator speed on the nucleation rate and particle size distribution. The agitator speeds used for the experiments were 300, 400, 500, and 600 rpm, respectively, with a mean residence time of 1175 s. The experimental particle size distributions were determined using the on-line Lasentec FBRM instrument showing a shift to the smaller particle sizes due to the increase in the agitation rate and hence secondary nucleation and attrition (Figure 6). gPROMS was used to simulate the steady-state continuous crystallization processes at different agitator rates using eq 11 to describe the total nucleation rates. The volume mean particle size (L_{43}) predicted from gPROMS was then compared to experimental values at the various agitator rates and shows a good agreement (Figure 7).

In summary, process modelling and simulation using CFD and gPROMS was successfully used to provide valuable information with regards to the improved mass transfer and lower attrition and nucleation rates with larger mean particle size being observed with a flat blade impeller over the pitch blade impeller in a continuous crystallizer.

3.2. Case Study II: Laboratory-Scale Batch Cooling Crystallizer. In this case study, the unseeded batch crystallization of an organic fine chemical in a laboratory-scale batch cooling suspension crystallizer was evaluated. gPROMS is used to predict the particle size distribution using pitch blade and flat blade impellers described in section 3.1.1. Furthermore, the bulk temperature profiles are predicted using gPROMS and compared to experimental measurements.

3.2.1. Experimental Set-Up. A 0.5-L batch cooling crystallizer was used with two different impeller types. The two

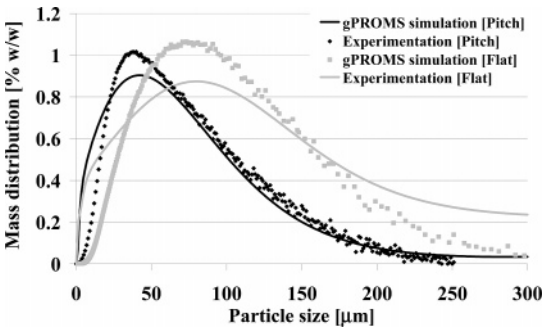

Figure 8. **Experimental and gPROMS-simulated batch-cooling crystal size distributions based on using pitch blade and flat blade impellers operating at 300 rpm.**

impeller types considered were a four-bladed 45° pitch blade impeller ($d_i = 45$ mm) and a two-bladed flat blade impeller ($d_i = 60$ mm). With a pitch blade impeller, three baffles were used, whereas no baffles were used with the flat blade impeller. The experiments were performed at an impeller velocity of 300 rpm using a 6% w/w solute concentration with the saturated solution at 60 °C being cooled to 10 °C at a rate of 0.5 °C min^{-1}. A Lasentec FBRM instrument was used on-line and in real time to monitor the chord length distribution, and a digital thermocouple was used to measure the bulk temperature profile in the crystallizer.

3.2.2. gPROMS Simulation Predictions. Figure 8 shows the particle size distributions produced using both flat blade and pitch blade impellers with the crystallizer equipped with the flat blade impeller producing larger particle sizes. gPROMS was used to simulate the particle size distributions using pitch blade and flat blade impellers, and these were compared to the experimental particle size distribution (Figure 8). The crystallization kinetics for growth and nucleation were combined with the population, mass, and energy balance (with estimated heat transfer coefficient using eq 7) within the gPROMS-modelling environment. The experimental and predicted volume mean sizes were determined to be 50 and 40 μm, respectively, for the batch crystallizer equipped with a pitch blade impeller and 75 and 65 μm for the batch crystallizer equipped with a flat blade impeller. The crystallization kinetics determined from the MSMPR crystallizations were adopted for batch cooling crystallization predictions leading to the particle size being underestimated. Furthermore, the energy balance is based on an estimated heat transfer coefficient including the enthalpy of crystallization and was used to simulate the temperature distribution in the batch crystallizer during cooling. Figure 9 shows the predicted and experimental bulk temperature profiles including the coolant (oil) temperature profile during the batch cooling crystallization equipped with a pitch blade impeller. The gPROMS simulation temperature profile reproduces the experimental temperature profile and clearly shows the enthalpy release due to primary nucleation resulting in a slight rise in temperature at 35 °C.

3.3. Case Study III: Scale-Up CFD Simulations of Batch Crystallizers. In this final case study, qualitative scale-up CFD simulations were carried out using constant agitator speed and constant power input per unit mass as scale-up criteria.

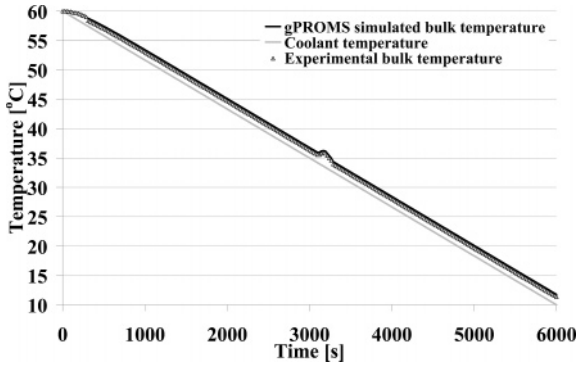

Figure 9. **Experimental and gPROMS-simulated bulk temperature profiles based on a linear cooling profile.**

3.3.1. Scale-Up Using Constant Agitator Speed. CFD solid−liquid phase simulations based on a geometrically similar 5-L and 25-L batch crystallizers equipped with a Ruston turbine impeller operating at an agitator speed of 300 rpm were considered for the constant agitator speed scale-up criteria. A dilute solid suspension of 5% v/v with a mean particle size of 200 μm was used for the simulations.

Figure 10 shows the solids concentration (vertical) profile for the 5-L and 25-L batch crystallizers. CFD simulations predict that the solids concentration profile is homogeneously distributed throughout the vessel in the 25-L vessel. There is also a disappearance of the clear mother liquor region, which is observed in the 5-L vessel. The difference observed in the solids concentration profile occurs even though the pumping volumetric flow rate per unit volume is constant upon scale-up. This is, however, due to the increase in the power input, tip speed and Reynolds number. The multiple frames of reference (MFR) technique was used to model the impeller rotation in the agitated vessels until steady state was achieved for the flow rates and solid fraction distribution.

On the basis of the Zwietering correlation, the just suspended speed is estimated at 260 and 165 rpm in the 5-L and 25-L vessels with a homogeneous suspension being achieved at 390 and 250 rpm. The just suspended speeds concur with the CFD predictions. On the basis of a constant volumetric pumping rate, which is estimated from CFD, we should expect to see similar macromixing performance or circulation times upon scale-up. The macromixing times are calculated using eq 5 and are 4.2 and 4 s for the 5-L and 25-L vessels, respectively.

Hence, with this scale-up criterion, the mixing becomes more homogeneous with improved mass transfer, but the increase in power requirements is not energy efficient and more importantly will result in excessive fines production due to increased attrition because the energy dissipation rate increases significantly. This will affect filtration times and present problems with downstream process operations and formulation. Hence, scale-up with constant agitator speed is not recommended.

3.3.2. Scale-Up Using Constant Specific Power Input per Unit Mass. The importance of the local energy dissipation rate (particularly in the impeller region) and hence the specific power input for a batch cooling crystallization process is directly linked to the attrition and secondary nucleation rates. Table 2 shows the local energy dissipation rates at the vessel wall adjacent to the impellers including other turbulence characteristics on various scales of operation in agitated vessels equipped with a pitch blade and Rushton turbine impeller. CFD simulations predict that, when scaling up with the application of constant power input per unit mass, there is a competing mechanism expected between macromixing and micromixing phenomena that can influence the crystallization kinetics and, hence, product performances. CFD simulations were carried out on 1-L, 5-L, and 25-L agitated vessels that exhibited geometric similarity (ratios maintained constant with scale-up including working volumes) using a constant power input per unit mass.[21] The vessels equipped with a pitch blade and Rushton turbine impeller show that the effects of micromixing on a localized scale are reduced upon scale-up and as a consequence of the local energy dissipation profiles not being identical. The reason for this is that energy is dissipated over larger distances due to the increase in vessel size and volume.The CFD predictions of the solid−liquid phase show that, although the macromixing times increase with scale (Table 2), the solids concentration profiles are more homogeneous.

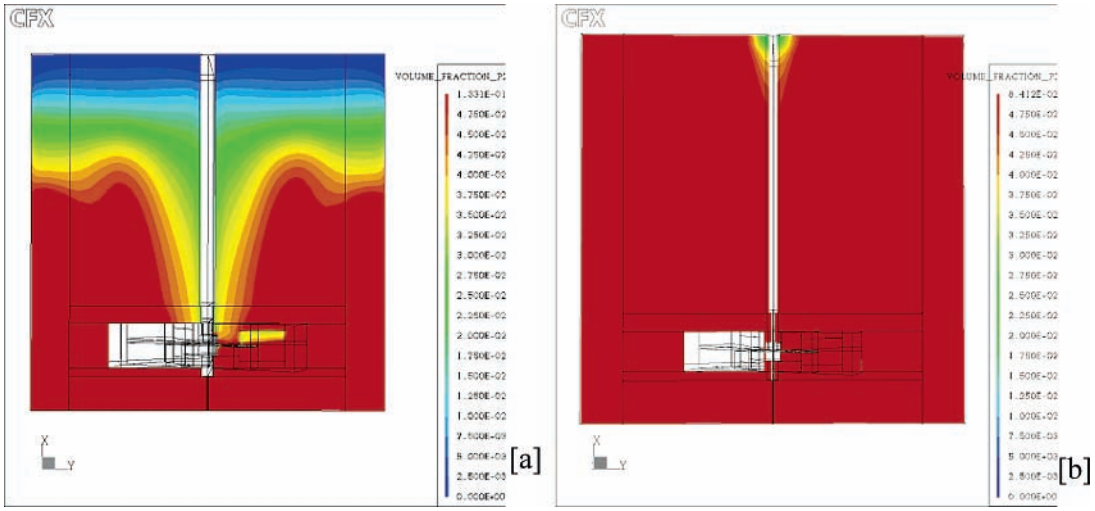

Figure 10. **Solids concentration vertical profile based on a maximum volume hold-up of 5% v/v with a mean particle size of 200 μm: (a) 5-L and (b) 25-L.**

Table 2. **Mixing and turbulence characteristics using a constant power input per unit mass [0.12 W kg^{-1}] on different scales of operation**

	Rushton turbine impeller					pitch blade impeller				
size [L]	speed [rpm]	*Re*	ϵ_{loc} [W/kg]	ϵ_{max} [W/kg]	t_{circ} (s)	speed [rpm]	*Re*	ϵ_{loc} [W/kg]	ϵ_{max} [W/kg]	t_{circ} (s)
1	300	3370	0.38	39	3.18	460	5121	0.71	61	2.24
5	289	6920	0.29	24	4.50	450	10800	0.55	44	2.96
25	201	13799	0.19	18	6.56	313	21500	0.29	27	4.30

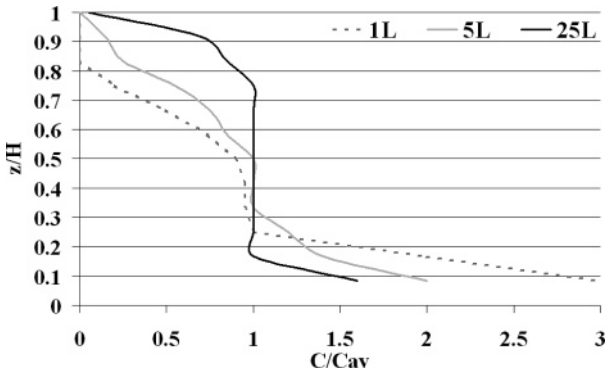

Figure 11. **Normalised solids concentration profile as a function of normalised vessel height using a solids concentration (C_{av}) of 5% v/v at different vessel scales using a constant power input per unit mass (pitch blade impeller).**

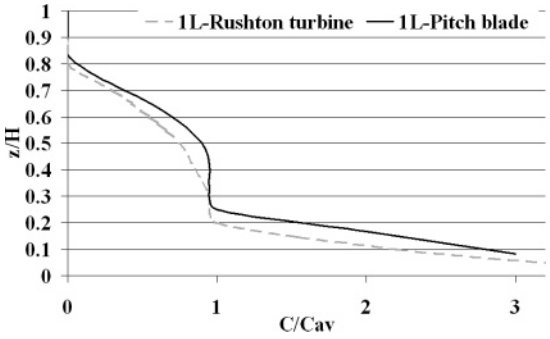

Figure 12. **Normalised solids concentration profile as a function of normalised vessel height using a solids concentration (C_{av}) of 5% v/v at the same vessel scale using a Rushton turbine and pitch blade impeller at constant specific power input per unit mass.**

Figure 11 and Figure 12 show the predicted normalized solids concentration (vertical profile) as a function of vessel height (normalized), for a dilute suspension of 5% v/v with a mean particle size of 200 μm for the different scales of operation and impeller types. This is attributed to the increase in the tip speed and Reynolds number with an increase in scale, producing higher volumetric flow rates within the batch-agitated crystallizers. The impeller type used also influences the micromixing and macromixing effects using the same constant power input per unit mass. The pitch blade impeller operates at higher impeller frequencies producing higher tip speeds and volumetric pumping rates than does a batch crystallizer equipped with a Rushton turbine. This results in reduced macromixing times at the same vessel scale (Table 2).

The significance of these observations in terms of a batch-cooling suspension crystallization process is that, upon scale-up with a constant power input per unit mass, the product performance and quality could be improved significantly, providing that an agitation speed that produces a homogeneous suspension and minimises the energy dissipation and shear stress is used. However, the influence of heat transfer has not been considered and will be discussed in the following section.

Using a constant specific power input per unit mass being used as a scale-up criterion results in reduced heat transfer coefficients being estimated for both pitch blade and Rushton turbine impellers. CFD heat transfer simulations were carried out based on using an estimated liquid side heat transfer coefficient using an empirical correlation known as the Nusselt number using eq 8.

The main aim of this part of the study was to use CFD simulations to identify "cooling zones" or surfaces where steep gradients in the temperature distribution are likely to occur within a batch-cooling crystallizer. Gradients in the temperature distribution affect the supersaturation profiles and therefore the crystallization kinetics and product performance. In comparison with the temperature distribution, higher levels of supersaturation correspond to lower temperatures. The shapes of these distributions are not identical as proposed by Yang et al.[47,50] The temperature mainly determines the supersaturation distribution, but it is also affected by the concentration distribution of the mother liquor and the particle size distribution. Therefore, the combined effects of the mixing and heat transfer influence the supersaturation profiles within a batch crystallizer. A linear cooling profile was used in the CFD simulations. A saturated solution at 80 °C was cooled to 20 °C at −1 °C min^{-1}. Upon scale-up from a 1-L to 25-L scale, heat transfer becomes less efficient when cooling occurs, resulting in higher temperatures being observed within the crystallizers at different time intervals. Figure 13 shows the bulk temperature profiles produced in the 1-L, 5-L, and 25-L batch crystallizers equipped with a Rushton turbine impeller. The reason for this is that the local energy dissipation distribution is reduced upon scale-up as discussed previously, and hence less efficient heat removal occurs at a particular linear cooling rate. Figure 14 shows the CFD predicted temperature distribution in the 1-L, 5-L, and 25-L batch crystallizer equipped with a Rushton turbine impeller. A uniform bulk temperature distribution is observed; however, in the upper

(47) Yang, G.; Louhi-Kultanen, M.; Kallas, J. *Chem. Eng. Trans.* **2002**, *1*, 83−88.
(48) Bezzo, F.; Macchietto, S.; Pantelides, C. C. *Comput. Chem. Eng.* **2004**, *28*, 4, 501−511.
(49) Bezzo, F.; Macchietto, S.; Pantelides, C. C. *Comput. Chem. Eng.* **2004**, *28*, 4, 513−525.
(50) Kougoulos, E.; Jones, A. G.; Wood-Kaczmar, M. W. *J. Cryst. Growth* **2005**, *273*, 3−4, 529−534.

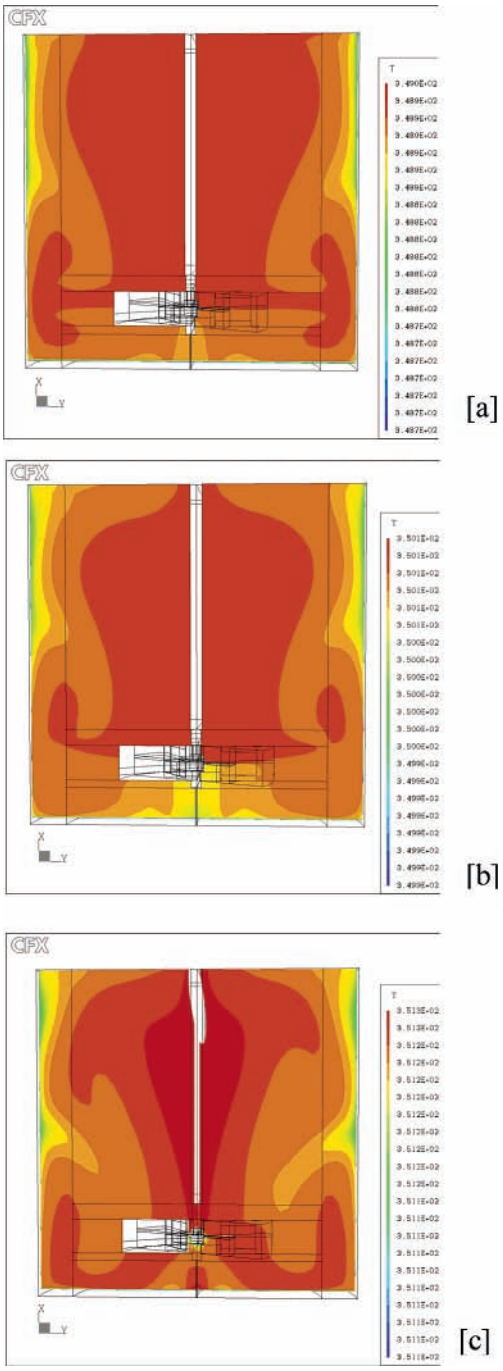

Figure 13. **Localised temperature distribution (vertical profile) after 360 s CFD simulation: (a) 1-L, (b) 5-L, (c) 25-L.**

regions of the crystallizers less efficient heat transfer occurs, resulting in cooling zones or surfaces. The temperature difference between the bulk and the cooling zones is 0.4 °C. The type of impeller used also influences the temperature distribution.

The less efficient heat transfer upon scale-up has a few implications on crystallization process development scale-up based on constant power input per unit mass. The process batch time must be increased upon scale-up to achieve the same degree of under cooling. This will result in different supersaturation profiles and hence different crystallization kinetics and particle size distributions. The cooling rate can be increased to compensate for the increase in scale of

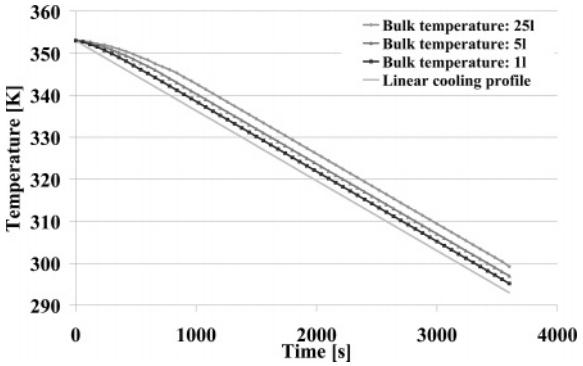

Figure 14. **CFD simulated bulk temperature profiles on different scales of operation.**

operation, but this may result in encrustation effects, particularly in poorly mixed zones such as the cooling zones. This will increase agglomeration, influence the crystal morphology, and produce wider particle size distributions. The agitation rate can be increased to improve heat removal, but this may increase the number of fines produced, which will decrease the filtration performance and influence downstream processing

From CFD predictive simulations there is a competing mechanism between macromixing, shear and energy dissipation (micromixing) including heat transfer upon scale-up, leading to the failure of common scale-up criteria used. To account for the influence of these phenomena described, it is necessary to implement a compartmentalisation approach to facilitate the scale-up of batch-cooling suspension crystallization processes. A previous contribution[21] gives a detailed approach to using compartmentalisation. It involves determining hydrodynamic information from CFD and coupling it with kinetics and solubility and optimising the process to ensure efficient mixing and heat transfer with minimisation of fines production such that an improved product performance and quality are achieved.

4. Conclusions

CFD allows an engineering insight to be introduced to determine the influence of hydrodynamics within agitated vessels. The effects of scale-up on the mixing, energy dissipation, and heat transfer using different impeller configurations and operating conditions was successfully analysed using CFD. CFD predicts that, when using constant agitator speed per unit mass, suspension mixing improves with a reduction in energy dissipation and shear distribution. This should allow for reduced breakage and secondary nucleation and more homogeneous suspensions being produced. However, the heat transfer becomes less efficient, and this may result in increased agglomeration due to encrustation effects. gPROMS is a powerful process-modelling tool for crystallization and was used to successfully predict the particle size distribution based on using crystallization kinetics and solubility for both batch and continuous laboratory crystallizers.

Acknowledgment

We thank GlaxoSmithKline pharmaceuticals for allowing part of this research to be carried out at the research and

development facilities at Stevenage, United Kingdom, and for financial support via an EPSRC Industrial Case Award.

Nomenclature

N	impeller rotational speed, [rps or rpm]
d	impeller diameter, [m]
D	impeller diameter, [m]
Po	power number, [-]
P	power input, [W]
M	torque, [N m^{-1}]
Q_p	pumping volumetric flowrate, [m^3 s^{-1}]
C_p	specific heat capacity, [kJ kg^{-1} K^{-1}]
k	thermal conductivity, [W m^{-1} K^{-1}]
h	heat transfer coefficient, [W m^{-2} K^{-1}]
C	concentration, [kg kg^{-1}]
T	temperature, [K]
G	growth rate, [m s^{-1}]
L	particle size, [μm or m]
k_g	growth rate coefficient, [m s^{-1}]
B_{TOT}	total nucleation rate, [m^{-3} s^{-1}]
M_T	suspension density, [kg m^{-3}]
g	gravitational acceleration, [m s^{-2}]
s	impeller constants, [-]
X	solids mass fraction, [-]
d_p	mean particle diameter, [m]
V	crystallization volume, [m^3]
Fl	flow number, [-]
Re	Reynolds number $= \rho_f N D_i / \mu$, [-]
Pr	Prandtl number $= C_p \mu / k$, [-]
Greek letters	
ρ	fluid density, [kg m^{-3}]
μ	viscosity, [Pa s^{-1}]
σ	relative supersaturation, [-]
ϵ	energy dissipation rate, [W kg^{-1}]
$\Delta\rho$	difference between crystalline and fluid density ($\rho_s - \rho_f$), [kg m^{-3}]
ν	kinematic viscosity, [Ns m kg^{-1}]
Subscripts	
p	pumping
w	wall
av	average
eq	equilibrium
i	impeller

Received for review February 20, 2006.

OP060039+